

RSC Advances



This is an *Accepted Manuscript*, which has been through the Royal Society of Chemistry peer review process and has been accepted for publication.

Accepted Manuscripts are published online shortly after acceptance, before technical editing, formatting and proof reading. Using this free service, authors can make their results available to the community, in citable form, before we publish the edited article. This *Accepted Manuscript* will be replaced by the edited, formatted and paginated article as soon as this is available.

You can find more information about *Accepted Manuscripts* in the [Information for Authors](#).

Please note that technical editing may introduce minor changes to the text and/or graphics, which may alter content. The journal's standard [Terms & Conditions](#) and the [Ethical guidelines](#) still apply. In no event shall the Royal Society of Chemistry be held responsible for any errors or omissions in this *Accepted Manuscript* or any consequences arising from the use of any information it contains.

Cite this: DOI: 10.1039/c0xx00000x

www.rsc.org/xxxxxx

ARTICLE TYPE

3-Substituted 6-oxoverdazyl bent-core nematic radicals: synthesis and characterization

Sylvia Ciastek,^a Marcin Jasiński,^a and Piotr Kaszyński^{a,b,c,*}

Received (in XXX, XXX) Xth XXXXXXXXX 20XX, Accepted Xth XXXXXXXXX 20XX

DOI: 10.1039/b000000x

A series of bent-core derivatives of 6-oxoverdazyls **1[12]** was synthesized and mesogenic properties were investigated in the pure form and in binary mixtures. Results demonstrate that the effectiveness of the C(3) substituent in nematic phase stabilization follows the order: COOMe > *m*-FC₆H₄ > Ph > Thienyl > *o*-FC₆H₄, which is consistent with steric parameters established with DFT computational methods and opposite to the order of the appearance of a re-entrant isotropic phase. The effect of alkyl chain elongation on mesogenic properties and the effect of C(3) substituent on electronic absorption spectra are also investigated.

Introduction

There is growing interest in liquid crystalline stable radicals as potential organic semiconductors and also materials for spintronics and fundamental studies of spin-spin interactions in organized media.¹⁻⁴ In this context, we have demonstrated 6-oxoverdazyl to be a suitable paramagnetic core element of mesogenic compounds and reported discotics bearing alkoxy^{5,6} and alkylsulfanyl substituents.⁷⁻⁹ These mesogenic radicals exhibit 3-dimensional columnar hexagonal phases up to 130 °C and substantial hole mobility of about 10⁻³ cm²V⁻¹s⁻¹.^{5,7} In search for new types of supramolecular architectures and hence types of intermolecular interactions, we turned to bent-core derivatives in which the 6-oxoverdazyl is the central angular paramagnetic element. We prepared series **1[n]a** containing the CF₃ group at the C(3) head position and demonstrated rich polymorphism, photo-induced ambipolar charge transport, and linear reorientation of optical axis in electric field in the series.¹⁰

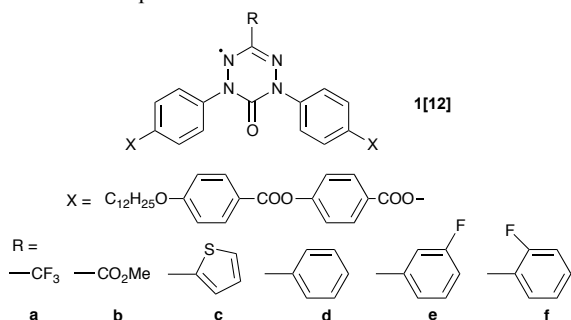


Fig 1. The structure of bent-core 6-oxoverdazyls **1[12]**.

It has been demonstrated that chemical modifications of the

head position in bent-core compounds affects their electronic properties and mesogenic behavior.^{11,12} For this reason, we set out to investigate verdazyl derivatives containing a functional group at the C(3) position that can be modified chemically. We also envisioned a substituent with an extended π system for modification of the electronic structure of the heterocycle and intermolecular π - π interactions. Here we report a series of derivatives **1[12]** containing carboxyl group (**1[12]b**) and also thienyl (**1[12]c**) and phenyl (**1[12]d**) rings (Fig. 1). We also investigate steric and polar effects of substitution of the phenyl ring with fluorine (**1[12]e** and **1[12]f**), and alkyl chain elongation (**1[16]c** and **1[16]d**) on phase properties. The new compounds are investigated in the pure form and as binary mixtures with **1[12]a**, and results are rationalized with the help of DFT calculations.

Results and discussion

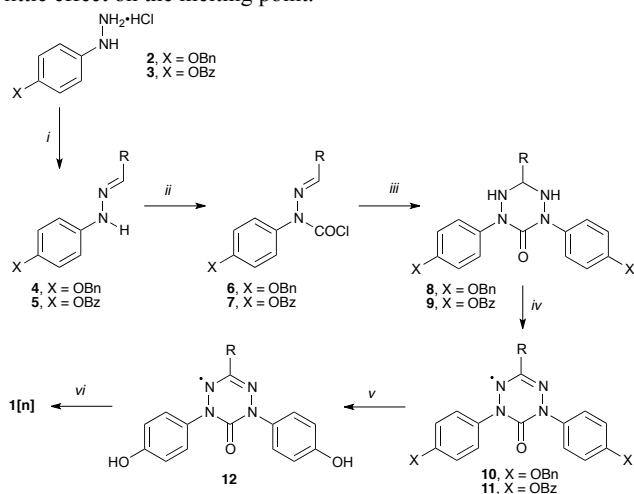
Synthesis

The preparation of bent-core derivatives **1[n]** follows the Milcent protocol¹³ and general functional group interconversion methods¹⁴ for 6-oxoverdazyls (Scheme 1), as was reported earlier for **1[n]a**.¹⁰ Thus, reactions of 4-substituted phenylhydrazine hydrochlorides **2** and **3** with appropriate aldehydes gave crude hydrazones **4b** and **5c-5f**, which were converted to carbamoyl chlorides **6b** and **7c-7f**, respectively, upon treatment with triphosgene in the presence of pyridine. After purification, the chlorides were reacted with appropriate arylhydrazine **2** or **3** in hot ethanol to give tetrazines **8b** and **9c-9f**, respectively. The crude tetrazines were subsequently oxidized to radicals **10b** and **11c-11f**, under PTC reaction conditions using K₃Fe(CN)₆ (*Method A*) or NaO₄ (*Method B*). The resulting 6-oxoverdazyl radicals were converted into the corresponding phenols **12b-12f** by catalytic debenzoylation (benzyl ether **10b**) or basic hydrolysis (benzoates **11c-11f**). The diphenols were acylated with appropriate acid chlorides **13[n]**^{15,16} in the presence of DMAP to provide compounds **1[n]** in yields of about 70%.

Thermal analysis

Analysis of series **1[12]** by optical (POM) and thermal (DSC) methods revealed that all compounds melt above 130 °C and only three out of six derivatives form a mesophase (Table 1). Thus, methoxycarbonyl derivative **1[12]b** and the previously reported CF₃ derivative **1[12]a** exhibit an enantiotropic nematic phase, while the *m*-fluorophenyl **1[12]e** forms a monotropic nematic

phase (Fig. 2a). The overall stability of the nematic phase follows the order $m\text{-FC}_6\text{H}_4 > \text{COOMe} > \text{CF}_3$ and the re-entrant isotropic phase was observed only in the CF_3 derivative **1[12]a**. Extension of the alkyl chain in the 3-thienyl and 3-phenyl derivatives did not induce mesogenic behavior in **1[16]c** and **1[16]d**, and had little effect on the melting point.



Scheme 1. Preparation of 6-oxoverdazyls **1[n]**. Reagents and conditions: (i) RCHO or $\text{RCH}(\text{OH})_2$; (ii) $\text{CO}(\text{OCCl}_3)_2$, pyridine, CH_2Cl_2 , rt; (iii) hydrazine hydrochloride **2** or **3**, Et_3N , EtOH , $60\text{ }^\circ\text{C}$; (iv) *Method A*: $\text{K}_3\text{Fe}(\text{CN})_6$, Na_2CO_3 , $[\text{Et}_4\text{N}]^+\text{Br}^-$ (cat.), $\text{CH}_2\text{Cl}_2\text{-H}_2\text{O}$, rt; or *Method B*: NaIO_4 , $[\text{Et}_4\text{N}]^+\text{Br}^-$ (cat.), $\text{CH}_2\text{Cl}_2\text{-H}_2\text{O}$, rt; (v) for $\text{X} = \text{OCOPh}$: KOH (0.1M in MeOH), CH_2Cl_2 ; for $\text{X} = \text{OBn}$: H_2 (3 atm), Pd/C , THF-EtOH ; (vi) $\text{C}_{10}\text{H}_{2n+1}\text{C}_6\text{H}_4\text{COOC}_6\text{H}_4\text{COCl}$ (**13[n]**), DMAP , CH_2Cl_2 , rt.

Table 1. Thermal properties of pure compounds and binary mixtures.^a

compound	Transition temperatures / $^\circ\text{C}$	Virtual transition temperatures / $^\circ\text{C}$ ^b	
		$[\text{T}_{\text{NI}}]$	$[\text{T}_{\text{Nre}}]$
1[12]a ^c	Cr 136.9 (I_{re} 121.6) ^d N 152.3 I ^e	–	–
1[12]b	Cr 139 N 161 I ^f	231	^g
1[12]c	Cr 153 I	138	136
1[12]d	Cr 157 I	163	139
1[12]e	Cr 177 (N 169) I	194	110
1[12]f	Cr 155 I	82	144
1[16]c	Cr 149 I	91	150
1[16]d	Cr 160 I	102	140

^a Cr = crystal, N = nematic, I and I_{re} = isotropic. ^b Extrapolated from ~ 10 mol% solutions in **1[12]a**; $[\text{T}_{\text{NI}}]$ linear extrapolation, $[\text{T}_{\text{Nre}}]$ nonlinear ($x^{1/2}$) extrapolation. See the ESI for details. ^c Ref.¹⁰. ^d Monotropic transition. ^e Peak transition temperatures. ^f Decomposition. ^g Not observed.

In order to understand the broader impact of the C(3) substituent on mesogenic properties, all derivatives were investigated as low concentration additives (~ 10 mol%) to **1[12]a**. Results demonstrate that all mixtures exhibit an enantiotropic nematic phase (N) and all, except for **1[12]b**–**1[12]a**, show a re-entrant isotropic phase (I_{re}), as shown for a **1[12]d**–**1[12]a** mixture in Figs. 2 and 3. Linear extrapolation of

the $\text{N} \rightarrow \text{I}$ and parabolic extrapolation^{10,17} of the $\text{N} \rightarrow I_{\text{re}}$ transition temperatures gave virtual temperatures $[\text{T}_{\text{NI}}]$ and $[\text{T}_{\text{Nre}}]$, respectively, shown in Table 1. Analysis of the results indicates that the effectiveness of the C(3) substituent in nematic phase stabilization follows the order: $\text{COOMe} > m\text{-FC}_6\text{H}_4 > \text{Ph} > \text{Thienyl} > o\text{-FC}_6\text{H}_4$. Not surprisingly, the virtual $\text{N} \rightarrow I_{\text{re}}$ transition temperatures follow the exactly opposite order, and substituents that most stabilize the nematic phase also most suppress the re-entrant isotropic phase.

Elongation of the alkyl chain significantly suppresses the virtual $\text{N} \rightarrow \text{I}$ transition, and the effect is stronger for the Ph derivative **1[16]d** than for the thienyl analogue **1[16]c**.

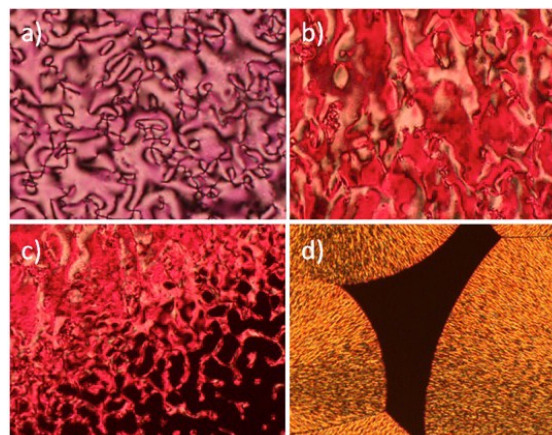


Fig. 2 Schlieren texture of nematic phase (a) for **1[12]e** on slow cooling from the isotropic phase, and a sequence of photomicrographs taken upon cooling of a 8.5 mol% solution of **1[12]d** in **1[12]a**: nematic phase (b), re-entrant isotropic phase growing from the nematic phase (c), and crystalline phase growing from I_{re} (d).

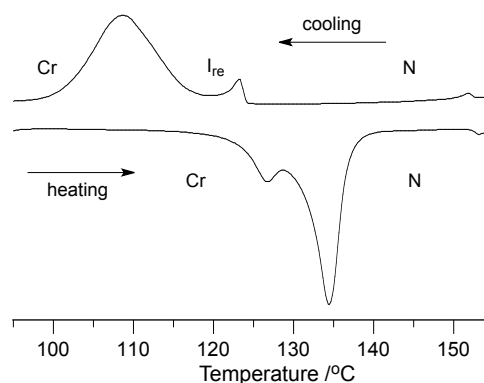


Fig. 3. DSC trace for a 8.5 mol% solution of **1[12]d** in **1[12]a**.

In an attempt to generate a wide temperature range nematic material with broad absorption in the visible range (*vide infra*), three-component mixtures of 3-thienyl, 3-phenyl, and 3- CF_3 derivatives were briefly investigated. Thus, addition of a nearly equimolar mixture of **1[12]c** and **1[12]d** to **1[12]a**, as the nematic host, in a 1:4 ratio gave a material with nematic phase range of $131\text{--}150\text{ }^\circ\text{C}$ and transition to I_{re} at $123\text{ }^\circ\text{C}$. Increasing of the content of the 3-aryl components to 1:1 ratio with **1[12]a** modestly suppressed the melting point to $125\text{ }^\circ\text{C}$ and significantly destabilized the nematic phase by 12 K. Also the re-entrant I_{re} phase was suppressed by 19 K in favour of the supercooled

nematic phase. Further increase of the ratio to 2:1 gave a nonhomogenous material with a high melting point of 142 °C and without an enantiotropic nematic phase.

Molecular modelling

For a better understanding of properties of derivatives **1[n]**, molecular and electronic structures of diphenols **12** set at the pseudo C_2 symmetry were investigated at the CAM-B3LYP/6-31G(2d,p) level of theory.

The resulting equilibrium structures, shown in Fig. 4 for **12b** and **12c**, are close to that obtained experimentally for 1,3,5-triphenyl-6-oxovedazyl.¹⁸ The 4-hydroxyphenyl rings are twisted off the co-planarity with the verdazyl ring and dihedral angles $N(2)-N(1)-C_{Ph}-C_{Ph}$ and $C(6)-N(1)-C_{Ph}-C_{Ph}$ are $33.9 \pm 1.0^\circ$ and $40.1 \pm 0.9^\circ$, respectively. The substituent at the C(3) position also lacks coplanarity with the heterocycle, and the dihedral angle θ is smallest for the thienyl derivative **12c** (3.3° , Table 2, Fig. 4) and the largest, as expected, for the *o*-FC₆H₄- derivative **12f** (30.2°).

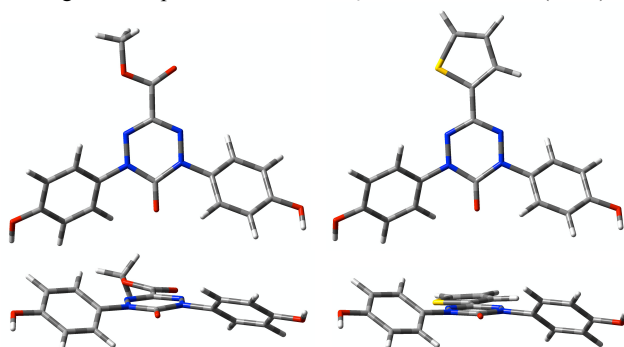


Fig. 4. Two views of equilibrium pseudo C_2 symmetry geometries for **12b** (left) and **12c** (right) obtained at the CAM-B3LYP/6-31G(2d,p) level theory.

A comparison of the results in Tables 1 and 2 demonstrates that the large twist angle θ of 30.2° calculated for **12f** correlates with the exceptionally low $[T_{Ni}]$ (82°C) and particularly high $[T_{Nire}]$ values (144°C) found for **1[12]f** derivative (Table 1). On the other hand, a relatively low $[T_{Ni}]$ value observed for the thienyl derivative **1[12]c** (138°C) despite a high degree of coplanarity ($\theta = 3.3^\circ$), is presumably related to the large size of the sulphur atom. Conversely, very high $[T_{Ni}]$ value for derivative **1[12]b** (231°C , Table 1) is related to the presence of a small planar semi-flexible polar COOMe group at the C(3) position with a moderate θ angle (11°).

Electronic absorption spectra

All radicals **1[n]** are intense red in solutions of typical organic solvents with the exception of thienyl derivatives **1[n]c**, which are dark green. Analysis of **1[12]a** in CH_2Cl_2 solutions demonstrated a broad, low intensity absorption band in the visible range with a maximum at 508 nm (Fig. 5). Replacement of the CF₃ group at the C(3) position with the thienyl in **1[12]c** resulted in broadening of the band and a strong bathochromic shift to $\lambda_{\text{max}} = 598$ nm. The *m*-FC₆H₄ derivative **1[12]e** absorbs in the intermediate range of wavelengths and shows two distinguishable maxima at $\lambda_{\text{max}} = 540$ and 566 nm. Thus, absorption of all three compounds effectively covers the range of 450-650 nm.

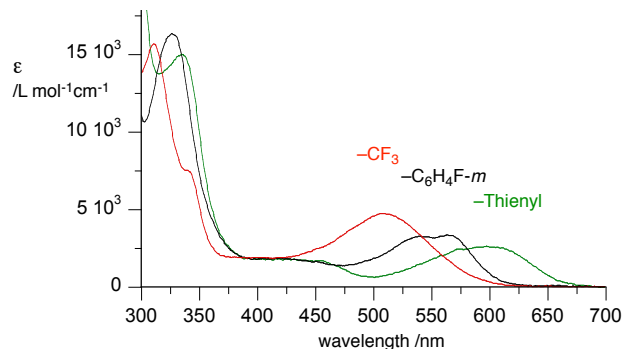


Fig. 5 Low energy portion of electronic absorption spectra for **1[12]a** (red), **1[12]c** (green) and **1[12]d** (black) in CH_2Cl_2 .

Results of TD-DFT calculations are consistent with experimental data and show a single, major ($f \sim 0.09-0.19$) low energy excitation in the visible range related mainly to the delocalized β -HOMO to the β -LUMO, concentrated on the verdazyl ring, transition (Fig. 6). Analysis of the theoretical values in Table 2 demonstrates that the wavelength of the lowest energy excitation follows the order: COOMe < *o*-FC₆H₄ < CF₃ ~ *m*-FC₆H₄ ~ Ph < Thienyl. Interestingly, the coplanarity of the Ph ring with the verdazyl appears to be important for modifying the HOMO-LUMO gap, as evident from comparison of the C(3)-*o*-FC₆H₄ (**12f**) and C(3)-*m*-FC₆H₄ (**12e**) derivatives (Table 2).

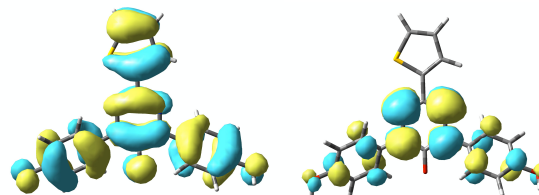


Fig. 6. B3LYP/6-31G(2d,p)-derived contours of β -HOMO (left) and β -LUMO (right) orbitals relevant to low energy excitations in **1[12]c**.

Table 2. Calculated substituent-verdazyl dihedral angle θ and the wavelength λ_{max} of the lowest energy electronic excitation for series **12**.

12	a	B	c	d	e	f
$\theta / ^\circ$ ^a	–	11.0	3.3	8.2	6.3	30.2
$\lambda_{\text{max}} / \text{nm}$ ^b	547	534	584	551	550	542

^a CAM-B3LYP/6-31G(2d,p) level of theory; ^b TD-B3LYP/6-31G(2d,p) //CAM-B3LYP/6-31G(2d,p) level of theory in CH_2Cl_2 dielectric medium.

EPR spectroscopy

EPR spectrum measured for dibenzyloxy derivative **10b** (Fig. 7) exhibits 9 broad lines with an average hyperfine coupling constant $a_N = 5.62$ G, which is typical for this class of verdazyls^[7] and consistent with spin density distribution in the molecule, as shown for **12c** in Fig. 7. The fundamental nine-line pattern is due to coupling to four quadrupolar ¹⁴N nuclei of the verdazyl system and the lines are broadened by minor coupling to hydrogen atoms of the attached aromatic rings.

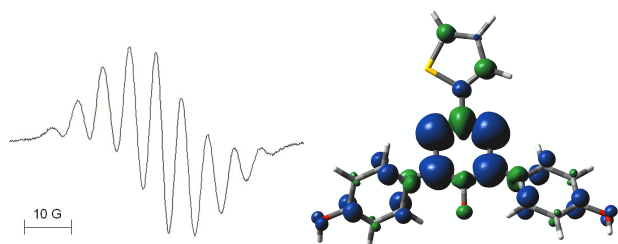


Fig. 7 Left: EPR spectrum of dibenzoyloxy **10b** recorded in benzene. Right: CAM-B3LYP/6-31G(2d,p) calculated spin density in **12c** (blue: alpha spin density, green: beta spin density).

5 Conclusions

Synthesis of several diphenols **12** and their acylation to form bent-core compounds **1[n]** has been demonstrated, which opens up possibilities of incorporation of these angular structural elements to other, more complex molecular and supramolecular systems. Analysis of series of bent-core derivatives **1[12]** revealed that some compounds form a rare nematic phase, but no ordered phases were observed even in higher homologues **1[16]**. Results show that the carboxy group in **1b** is a promising functionality for further manipulation with the supramolecular structure of the mesogens by esterification with more complex, including partially fluorinated alcohols. Investigation of series **1[n]** as ~10 mol% binary mixtures with nematogen **1[12]a** demonstrated that the trend in virtual $[T_{Ni}]$ is consistent with steric properties of the C(3) substituent obtained with DFT methods. Spectroscopic analysis revealed that electronic absorption of a ternary mixture of compounds **1[12]a**, **1[12]c**, and **1[12]d** covers most of the visible range, which makes it attractive for designing of materials for photovoltaics. Further investigation of derivatives of diphenols **12** and induction of banana phases is underway.

Computational details

Quantum-mechanical calculations were carried out using Gaussian 09 suite of programs.¹⁹ Geometry optimizations for unconstrained model compounds at the pseudo- C_2 symmetry were undertaken at the CAM-B3LYP/6-31G(2d,p) level of theory using tight convergence limits. Electronic excitation energies were obtained at the B3LYP/6-31G(2d,p)//CAM-B3LYP/6-31G(2d,p) level using time-dependent DFT calculations²⁰ supplied in the Gaussian package. Solvent effect on electronic excitations was included using the PCM model²¹ [keywords: SCRF(PCM, Solvent=CH2CL2)]. Equilibrium geometries and partial output data for TD-DFT calculations are provided in the ESI.

Experimental section

40 General

Solvents and reagents were purchased and used as received without further purification. Products were purified by flash chromatography on silica gel (230–400 mesh, Merck or Fluka). NMR spectra were recorded with Bruker AVIII 600 instrument. Chemical shifts are reported relative to solvent residual peaks (¹H NMR, $\delta = 7.26$ ppm [CDCl₃], $\delta = 2.50$ ppm [DMSO-*d*₆]; ¹³C

NMR, $\delta = 77.00$ ppm [CDCl₃], $\delta = 39.52$ ppm [DMSO-*d*₆]). Substitution patterns of the carbon atoms were determined with 2D NMR spectroscopy (COSY, HMQC) and are indicated as ¹³C NMR peak multiplicity. IR spectra were measured in KBr pellets or thin films. Mass spectrometry was performed with a Finnigan MAT-95 or a Varian 500-MS LC Ion Trap instrument. Melting points were determined in capillaries and are uncorrected. UV-vis spectra were recorded in spectroscopic grade CH₂Cl₂ at concentrations of $1\text{--}20 \times 10^{-6}$ and fitted to the Beer-Lambert law. If not stated otherwise, reactions were carried out under argon in a flame-dried flask with addition of the reactants by using syringe; subsequent manipulations were conducted in air. Synthesis and characterization of diphenol radicals **12** and other precursors and intermediates are provided in the ESI.

Preparation of binary mixtures: A mixture of known amounts of additive **1[n]** (~1 μmol) and the trifluoromethyl derivative **1[12]a** (~10 μmol) was placed in a small vial and 1,2-dichloroethane (0.1 mL) was added. The mixture was heated and stirred with a spatula at 50 °C (hot stage) to give a homogenous solution. The solvent was removed under stirring at about 80 °C and the resulting mixture was analyzed by POM to confirm homogeneity. Typically, each mixture was analyzed by DSC in 3 heating-cooling cycles and reproducible results (within 0.5 K) were averaged. The resulting transition peak temperatures were used to obtain virtual transition temperatures by linear ($[T_{Ni}] = 152.3 + a \cdot x_i$) or non-linear ($[T_{Nire}] = 121.6 + a \cdot x_i^{1/2}$) extrapolation to the pure compound ($x_i = 1$), as demonstrated elsewhere for similar mixtures.¹⁷

Synthesis of bent-core verdazyls 1[n]: To a mixture of diphenol radical **12** (0.20 mmol) and appropriate acid chloride **13[n]** (0.60 mmol) in 8 mL of dry CH₂Cl₂, solid DMAP (98 mg, 0.80 mmol) was added in one portion. The mixture was stirred at room temperature until the starting material and the by-product mono-acylated derivative were fully consumed (typically 2–5 min). The mixture was quenched with H₂O, diluted with CH₂Cl₂ and the organic layer was washed with 2% HCl (10 mL), 5% aq. NaHCO₃ (10 mL) and with H₂O (3 \times 25 mL). The organics were dried over MgSO₄, filtered, and the solvents were removed under reduced pressure. If not stated otherwise, the resulting crude product was flash chromatographed (SiO₂, CH₂Cl₂/EtOAc 95:5), and recrystallized 4–6 times from the CH₂Cl₂/EtOAc or CH₂Cl₂/MeCN mixtures.

1,5-bis{4-[4-(4-Dodecyloxybenzoyloxy)benzoyloxy]phenyl}-3-trifluoromethyl-6-oxoverdazyl (1[12]a): The synthesis and properties were described previously.¹⁰ UV-vis (CH₂Cl₂) λ_{max} (log ϵ) 269 (4.86), 311 (4.20), 341 (3.87), 508 (3.68).

1,5-bis{4-[4-(4-Dodecyloxybenzoyloxy)benzoyloxy]phenyl}-3-methoxycarbonyl-6-oxoverdazyl (1[12]b): Crude product was washed with several portions of cold methanol, then two times chromatographed (SiO₂, CH₂Cl₂/EtOAc 60:1 gradient to 30:1) and three times recrystallized from EtOAc/MeCN mixture to give red crystals (155 mg, 67%); IR (KBr) ν 1735 (C=O), 1605, 1510, 1255, 1200, 1160, 1060 cm⁻¹. Anal. Calcd for C₆₈H₇₇N₄O₁₃ (1157.5): C 70.51, H 6.70; found: C 70.58, H 6.94.

1,5-bis{4-[4-(4-Dodecyloxybenzoyloxy)benzoyloxy]phenyl}-6-oxo-3-(thien-2-yl)verdazyl (I[12]c): Green solid (165 mg, 70%), mp 153 °C; IR (KBr) ν 1735 (C=O), 1690, 1605, 1505, 1260, 1200, 1160, 1065 cm⁻¹; UV-vis (CH₂Cl₂) λ_{max} (log ϵ) 272.5 (4.92), 335 (4.18), 598 (3.42); MALDI-MS (*m/z*): 1205.5 (100, [M+Na]⁺), 1182.5 (15, [M+H]⁺), 1153.5 (47, [M-CO]⁺). Anal. Calcd for C₇₀H₇₇N₄O₁₁S (1181.5): C 71.10, H 6.56, N 4.74, S 2.71. Found: C 70.89, H 6.81, N 4.65, S 2.67.

1,5-bis{4-[4-(4-Hexadecyloxybenzoyloxy)benzoyloxy]phenyl}-6-oxo-3-(thien-2-yl)verdazyl (I[16]c): Green solid (163 mg, 63%), mp 148 °C; MALDI-MS (*m/z*) 1316.6 (32, [M+Na]⁺), 1294.7 (19, [M+H]⁺), 1265.6 (47, [M-CO]⁺). Anal. Calcd for C₇₈H₉₃N₄O₁₁S (1293.7): C 72.36, H 7.24, N 4.33, S 2.48. Found: C 72.38, H 7.26, N 4.35, S 2.45.

1,5-bis{4-[4-(4-Dodecyloxybenzoyloxy)benzoyloxy]phenyl}-6-oxo-3-phenylverdazyl (I[12]d): Crude product was flash chromatographed through a silica gel pad (CH₂Cl₂ gradient to CH₂Cl₂/EtOAc 20:1). Analytically pure sample was obtained after column chromatography (CH₂Cl₂/EtOAc 50:1) as a light red solid (181 mg, 77%); mp 157 °C; IR (KBr) ν 1670 (C=O), 1600, 1515, 1225 cm⁻¹. Anal. Calcd for C₇₂H₇₉N₄O₁₁ (1175.6): C 73.51, H 6.77, N 4.76; found: C 73.24, H 6.70, N 4.73.

1,5-bis{4-[4-(4-Dodecyloxybenzoyloxy)benzoyloxy]phenyl}-3-(3-fluorophenyl)-6-oxoverdazyl (I[12]e): Crude product was flash chromatographed (SiO₂, CH₂Cl₂/EtOAc 50:1) and then purified by column chromatography (SiO₂, CH₂Cl₂). Pure sample was obtained after recrystallization from a CH₂Cl₂/MeOH mixture, followed by two recrystallizations from a CH₂Cl₂/MeCN mixture to give violet solid (189 mg, 79%); UV-vis (CH₂Cl₂) λ_{max} (log ϵ) 266 (4.90), 327 (4.21), 540 (3.52), 564 (3.53); IR (KBr) ν 1740 (C=O), 1690, 1605, 1505, 1260, 1200, 1160, 1070 cm⁻¹; MALDI-MS (*m/z*) 1194.3 (22, [M+H]⁺), 1165.3 (100, [M-CO]⁺). Anal. Calcd for C₇₂H₇₈FN₄O₁₁ (1193.6): C 72.40, H 6.58. Found: C 72.23, H 6.50.

1,5-bis{4-[4-(4-Dodecyloxybenzoyloxy)benzoyloxy]phenyl}-3-(2-fluorophenyl)-6-oxoverdazyl (I[12]f): Crude product was chromatographed twice (SiO₂; first CH₂Cl₂/petroleum ether 10:1, then CH₂Cl₂/EtOAc 100:1) and recrystallized four times from a CH₂Cl₂/MeCN mixture to give a light violet solid (200 mg, 84%), mp 155 °C; IR (KBr) ν 3430 (OH), 1740 (C=O), 1690 (C=O), 1605, 1505, 1260, 1200, 1160, 1065 cm⁻¹. Anal. Calcd for C₇₂H₇₈FN₄O₁₁ (1193.6): C 72.40, H 6.58, N 4.69. Found: C 72.39, H 6.33, N 4.64.

Acknowledgements

This work was supported by National Science Center (2013/09/B/ST5/01230) and National Science Foundation (CHE-1214104) grants. M.J. also thanks The University of Łódź Foundation.

Notes and references

^a Faculty of Chemistry, University of Łódź, Tamka 12, 91-403 Łódź, Poland

^b Department of Chemistry, Middle Tennessee State University, Murfreesboro, TN, 37130, USA

^c Organic Materials Research Group, Department of Chemistry, Vanderbilt University, Nashville, TN 37235, USA. E-mail: piotr.kaszynski@vanderbilt.edu

† Electronic Supplementary Information (ESI) available: complete synthetic details for intermediates 4–12, mixture analysis, partial output data for TD-DFT calculations, and archive of optimized equilibrium geometries for 12. See <http://dx.doi.org/10.1039/b000000x/>

- Castellanos, S.; López-Calahorra, F.; Brillas, E.; Juliá, L.; Velasco, D. *Angew. Chem. Int. Ed.* **2009**, *48*, 6516-6519.
- Ravat, P.; Marszalek, T.; Pisula, W.; Mullen, K.; Baumgarten, M. *J. Am. Chem. Soc.* **2014**, *136*, 12860-12863.
- Ikuma, N.; Tamura, R.; Shimono, S.; Kawame, N.; Tamada, O.; Sakai, N.; Yamauchi, J.; Yamamoto, Y. *Angew. Chem. Int. Ed.* **2004**, *43*, 3677-3682.
- Ikuma, N.; Tamura, R.; Shimono, S.; Uchida, Y.; Masaki, K.; Yamauchi, J.; Aoki, Y.; Nohira, H. *Adv. Mater.* **2006**, *18*, 477-480.
- Jankowiak, A.; Pocięcha, D.; Monobe, H.; Szczytko, J.; Kaszyński, P. *Chem. Commun.* **2012**, *48*, 7064 - 7066.
- Jankowiak, A.; Pocięcha, D.; Szczytko, J.; Kaszyński, P. *Liq. Cryst.* **2014**, *41*, 1653–1660.
- Jankowiak, A.; Pocięcha, D.; Szczytko, J.; Monobe, H.; Kaszyński, P. *J. Am. Chem. Soc.* **2012**, *134*, 2465-2468.
- Jankowiak, A.; Pocięcha, D.; Szczytko, J.; Monobe, H.; Kaszyński, P. *J. Mater. Chem. C*, **2014**, *2*, 319-324.
- Jankowiak, A.; Pocięcha, D.; Szczytko, J.; Monobe, H.; Kaszyński, P. *Liq. Cryst.* **2014**, *41*, 385–392.
- Jasiński, M.; Pocięcha, D.; Monobe, H.; Szczytko, J.; Kaszyński, P. *J. Am. Chem. Soc.* **2014**, *136*, 14658–14661.
- Reddy, R. A.; Tschierske, C. *J. Mater. Chem.* **2006**, *16*, 907-961.
- Iglesias, W.; Jákli, A. In *Handbook of Liquid Crystals*; Goodby, J. W., Collings, P. J., Kato, T., Tschierske, C., Gleeson, H. F., Raynes, P., Eds.; Wiley-VCH: Mörlenbach, Germany, 2014; Vol. 8, p 799-817.
- Milcent, R.; Barbier, G.; Capelle, S.; Catteau, J.-P. *J. Heterocyc. Chem.* **1994**, *31*, 319-324.
- Jasiński, M.; Gerding, J. S.; Jankowiak, A.; Gębicki, K.; Romański, J.; Jastrzębska, K.; Sivaramamorthy, A.; Mason, K.; Evans, D. H.; Celeda, M.; Kaszyński, P. *J. Org. Chem.* **2013**, *78*, 7445-7454.
- Reddy, G. S. M.; Narasimhaswamy, T.; Jayaramudu, J.; Sadiku, E. R.; Raju, K. M.; Ray, S. S. *Aust. J. Chem.* **2013**, *66*, 667-675.
- Pocięcha, D.; Ohta, K.; Januszko, A.; Kaszyński, P.; Endo, Y. *J. Mater. Chem.* **2008**, *18*, 2978-2982.
- Jasiński, M.; Gębicki, K.; Kaszyński, P. *Liq. Cryst.* **2015**, *42*, 000.
- Neugebauer, F. A.; Fischer, H.; Krieger, C. *J. Chem. Soc. Perkin Trans. 2* **1993**, 535–544.
- Gaussian 09, Revision A.02, M. J. Frisch, G. W. Trucks, H. B. Schlegel, G. E. Scuseria, M. A. Robb, J. R. Cheeseman, G. Scalmani, V. Barone, B. Mennucci, G. A. Petersson, H. Nakatsuji, M. Caricato, X. Li, H. P. Hratchian, A. F. Izmaylov, J. Bloino, G. Zheng, J. L. Sonnenberg, M. Hada, M. Ehara, K. Toyota, R. Fukuda, J. Hasegawa, M. Ishida, T. Nakajima, Y. Honda, O. Kitao, H. Nakai, T. Vreven, J. A. Montgomery, Jr., J. E. Peralta, F. Ogliaro, M. Bearpark, J. J. Heyd, E. Brothers, K. N. Kudin, V. N. Staroverov, R. Kobayashi, J. Normand, K. Raghavachari, A. Rendell, J. C. Burant, S. S. Iyengar, J. Tomasi, M. Cossi, N. Rega, J. M. Millam, M. Klene, J. E. Knox, J. B. Cross, V. Bakken, C. Adamo, J.

Jaramillo, R. Gomperts, R. E. Stratmann, O. Yazyev, A. J. Austin, R. Cammi, C. Pomelli, J. W. Ochterski, R. L. Martin, K. Morokuma, V. G. Zakrzewski, G. A. Voth, P. Salvador, J. J. Dannenberg, S. Dapprich, A. D. Daniels, O. Farkas, J. B. Foresman, J. V. Ortiz, J. Cioslowski, and D. J. Fox, Gaussian, Inc., Wallingford CT, 2009.

(20) Stratmann, R. E.; Scuseria, G. E.; Frisch, M. J. *J. Chem. Phys.* **1998**, *109*, 8218-8224.

(21) Cossi, M.; Scalmani, G.; Rega, N.; Barone, V. *J. Chem. Phys.* **2002**, *117*, 43-54, and references therein.

(22) Donohoe, T. J.; Fishlock, L. P.; Procopiu, P. A. *Org. Lett.* **2008**, *10*, 285-288.